28

# Modeling Thermoregulation and Core Temperature in Anatomically-Based Human Models and Its Application to RF Dosimetry

Akimasa Hirata
*Nagoya Institute of Technology*
*Japan*

## 1. Introduction

There has been increasing public concern about the adverse health effects of human exposure to electromagnetic (EM) waves. Elevated temperature (1-2°C) resulting from radio frequency (RF) absorption is known to be a dominant cause of adverse health effects, such as heat exhaustion and heat stroke (ACGIH 1996). According to the RF research agenda of the World Health Organization (WHO) (2006), further research on thermal dosimetry of children, along with an appropriate thermoregulatory response, is listed as a high-priority research area. The thermoregulatory response in children, however, remains unclear (Tsuzuki *et al.* 1995, McLaren *et al.* 2005). Tsuzuki suggested maturation-related differences in the thermoregulation during heat exposure between young children and mothers. However, for ethical reasons, systemic work on the difference in thermoregulation between young children and adults has not yet been performed, resulting in the lack of a reliable thermal computational model.

In the International Commission on Non-Ionizing Radiation Protection (ICNIRP) guidelines (1998), whole-body-averaged specific absorption rate (SAR) is used as a metric of human protection from RF whole-body exposure. In these guidelines, the basic restriction of whole-body-averaged SAR is 0.4 W/kg for occupational exposure and 0.08 W/kg for public exposure. The rationale of this limit is that exposure for less than 30 min causes a body-core temperature elevation of less than 1°C if whole-body-averaged SAR is less than 4 W/kg (e.g., Chatterjee and Gandhi 1983, Hoque and Gandhi 1988). As such, safety factors of 10 and 50 have been applied to the above values for occupational and public exposures, respectively, to provide adequate human protection.

Thermal dosimetry for RF whole-body exposure in humans has been conducted computationally (Bernardi *et al*. 2003, Foster and Adair 2004, Hirata *et al*. 2007b) and experimentally (Adair *et al*. 1998, Adair *et al*. 1999). In a previous study (Hirata *et al*. 2007b), for an RF exposure of 60 min, the whole-body-averaged SAR required for body-core temperature elevation of 1°C was found to be 4.5 W/kg, even in a man with a low rate of perspiration. Note that the perspiration rate was shown to be a dominant factor influencing the body-core temperature due to RF exposure. The SAR value of 4.5 W/kg corresponds to a

safety factor of 11, as compared with the basic restriction in the ICNIRP guidelines, which is close to a safety margin of 10. However, the relationship between the whole-body-averaged SAR and body-core temperature elevation has not yet been investigated in children.
In this chapter, a thermal computational model of human adult and child has been explained. This thermal computational model has been validated by comparing measured temperatures when exposed to heat in a hot room (Tsuzuki *et al.* 1995, Tsuzuki 1998). Using the thermal computation model, we calculated the SAR and the temperature elevation in adult and child phantoms for RF plane-wave exposures.

## 2. Model and Methods

### 2.1 Human Body Phantom

Figure 1 illustrates the numeric Japanese female, 3-year-old and 8-month-old child phantoms. The whole-body voxel phantom for the adult female was developed by Nagaoka *et al.* (2004). The resolution of the phantom was 2 mm, and the phantom was segmented into 51 anatomic regions. The 3-year-old child phantom (Nagaoka *et al.* 2008) was developed by applying a free-form deformation algorithm to an adult male phantom (Nagaoka *et al.* 2004). In the deformation, a total of 66 body dimensions was taken into account, and manual editing was performed to maintain anatomical validity. The resolution of these phantoms was kept at 2 mm. For European and American adult phantoms, e.g., see the literatures by Dimbylow (2002, 2005) and Mason et al. (2000). These phantoms have the resolution of a few millimeter.

In Section 3.1, we compare the computed temperatures of the present study with those measured by Tsuzuki (1998). Eight-month-old children were used in her measurements.

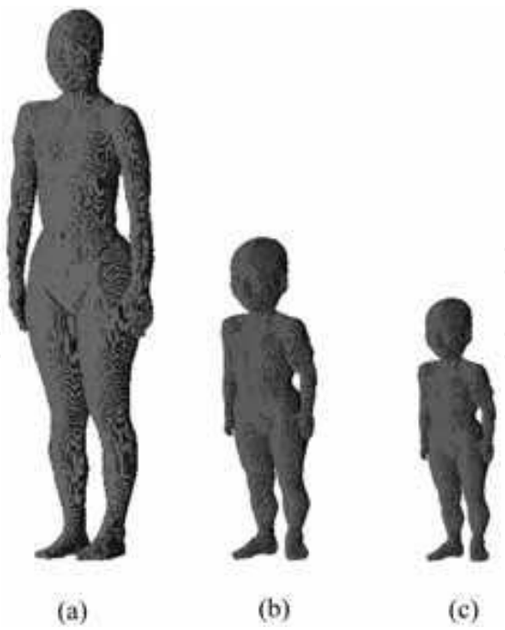


Fig. 1. Anatomically based human body phantoms of (a) a female adult, (b) a 3-year-old child, and (c) an 8-month-old child.

| | $H$ [m] | $W$ [kg] | $S$ [m²] | $S/W$ [m²/kg] |
|---|---|---|---|---|
| Female | 1.61 | 53 | 1.5 | 0.029 |
| 3 year old | 0.90 | 13 | 0.56 | 0.043 |
| 8 month old | 0.75 | 9 | 0.43 | 0.047 |

Table 1. Height, weight, and surface area of Japanese phantoms.

Thus, we developed an 8-month-old child phantom from a 3-year-old child by linearly scaling using a factor of 0.85 (phantom resolution of 1.7 mm). The height, weight, and surface area of these phantoms are listed in Table 1. The surface area of the phantom was estimated using a formula proposed by Fujimoto and Watanabe (1968).

### 2.2 Electromagnetic Dosimetry

The FDTD method (Taflove & Hagness, 2003) is used for calculating SAR in the anatomically based human phantom. The total-field/scattered-field formulation was applied in order to generate a proper plane wave. To incorporate the anatomically based phantom into the FDTD method, the electrical constants of the tissues are required. These values were taken from the measurements of Gabriel (1996). The computational region has been truncated by applying a perfectly matched layer-absorbing boundary. For harmonically varying fields, the SAR is defined as

$$\mathrm{SAR} = \frac{\sigma}{2\rho} |\mathbf{E}|^2 = \frac{\sigma}{2\rho}(|\hat{E}_x|^2 + |\hat{E}_y|^2 + |\hat{E}_z|^2) \tag{1}$$

where $\hat{E}_x$, $\hat{E}_y$, and $\hat{E}_z$ are the peak values of the electric field components, and σ and ρ are the conductivity and mass density, respectively, of the tissue.

### 2.3 Thermal Dosimetry

The temperature elevation in numeric human phantoms was calculated using the bioheat equation (Pennes 1948). A generalized bioheat equation is given as:

$$\begin{aligned} C(\mathbf{r})\rho(\mathbf{r})\frac{\partial T(\mathbf{r},t)}{\partial t} &= \nabla\cdot(K(\mathbf{r})\nabla T(\mathbf{r},t)) + \rho(\mathbf{r})SAR(\mathbf{r}) + A(\mathbf{r},t) \\ &\quad - B(\mathbf{r},t))(T(\mathbf{r},t) - T_B(\mathbf{r},t)) \end{aligned} \tag{2}$$

where $T(\mathbf{r},t)$ and $T_B(\mathbf{r},t)$ denote the temperatures of tissue and blood, respectively, $C$ is the specific heat of tissue, $K$ is the thermal conductivity of tissue, $A$ is the basal metabolism per unit volume, and $B$ is a term associated with blood perfusion. The boundary condition between air and tissue for Eq. (2) is expressed as:

$$-K(\mathbf{r})\frac{\partial T(\mathbf{r},t)}{\partial n} = H(\mathbf{r})\cdot(T_s(\mathbf{r},t) - T_e(t)) + S \quad \left(W, T_s(\mathbf{r},t)\right) \tag{3}$$

$$SW\left(\mathbf{r},T_s(\mathbf{r},t)\right)=P_{ins}+SW_{act}\left(\mathbf{r},T_s(\mathbf{r},t)\right) \tag{4}$$

where $H$, $T_s$, and $T_e$ denote, respectively, the heat transfer coefficient, the body surface temperature, and the air temperature. The heat transfer coefficient includes the convective and radiative heat losses. $SW$ is comprised of the heat losses due to perspiration $SW_{act}$ and insensible water loss $P_{ins}$. $T_e$ is chosen as 28°C, at which thermal equilibrium is obtained in a naked man (Hardy & Du Bois 1938).

In order to take into account the body-core temperature variation in the bioheat equation, it is reasonable to consider the blood temperature as a variable of time $T_B(\mathbf{r},t)=T_B(t)$. Namely, the blood temperature is assumed to be uniform over the whole body, since the blood circulates throughout the human body in 1 min or less (Follow and Neil 1971). The blood temperature variation is changed according to the following equation (Bernardi *et al*. 2003, Hirata & Fujiwara, 2009):

$$T_B(t)=T_{B0}+\int_t \frac{Q_{BT}(t)-Q_{BT}(0)}{C_B \rho_B V_B}\mathrm{d}t \tag{5}$$

where $C_B$ (= 4,000 J/kg·°C) is the specific heat, $\rho_B$ (= 1,050 kg/m$^3$) is the mass density, and $V_B$ is the total volume of blood. $V_B$ is chosen as 700 ml, 1,000 ml, and 5,000 ml for the 8-month-old and 3-year-old child phantoms and the adult phantom (ICRP 1975), respectively. $Q_{BT}$ is the rate of heat acquisition of blood from body tissues given by the following equation;

$$Q_{BT}(t)=\int_V B(t)(T_B(t)-T(\mathbf{r},t))dV. \tag{6}$$

Thorough discussion on blood temperature variation in the bioheat equation can be found in Hirata & Fujiwara (2009).

### 2.4 Thermal Constants of Human Tissues

The thermal constants of tissues in the adult were approximately the same as those reported in our previous study (Hirata *et al.* 2006a), as listed in Table 2. These are mainly taken from Cooper and Trezek (1971). The basal metabolism was estimated by assuming it to be proportional to the blood perfusion rate (Gordon *et al*. 1976), as Bernardi *et al.* did (2003). In the thermally steady state without heat stress, the basal metabolism is 88 W. This value coincides well with that of the average adult female. The basal metabolic rate in the 8-month-old and 3-year-old child phantoms were determined by multiplying the basal metabolic rate of the adult by factors of 1.7 and 1.8, respectively, so that the basal metabolism in these child phantoms coincides with those of average Japanese (Nakayama and Iriki 1987): 47 W and 32 W for 3-year-old and 8-month-old children. Similarly, based on a study by Gordon *et al.* (1976), the same coefficients were multiplied by the blood perfusion rate. The specific heat and thermal conductivity of tissues were assumed to be identical to those of an adult, because the difference in total body water in the child and adult is at most a few percent (ICRP 1975).

The heat transfer coefficient is defined as the summation of heat convection and radiation. The heat transfer coefficient between skin and air and that between organs and internal air are denoted as $H_1$ and $H_2$, respectively. Without heat stress, the following equation is maintained:

| tissue | $K$[W m$^{-1}$ $^{o}$C] | $C$[J kg$^{-1}$ $^{o}$C ] | $\rho$[kg m$^{-3}$] | $B$[W m$^{-3}$ $^{o}$C ] | $A$[W m$^{-3}$] |
|---|---|---|---|---|---|
| air | 0 | 0 | 0 | 0 | 0 |
| Internal air | 0 | 0 | 0 | 0 | 0 |
| skin | 0.27 | 3600 | 1125 | 1700 | 1620 |
| muscle | 0.40 | 3800 | 1047 | 2000 | 480 |
| fat | 0.22 | 3000 | 500 | 1500 | 300 |
| bone (cortical) | 0.37 | 3100 | 1990 | 3400 | 610 |
| bone (cancellous) | 0.41 | 3200 | 1920 | 3300 | 590 |
| nerve (spine) | 0.46 | 3400 | 1038 | 40000 | 7100 |
| gray matter | 0.57 | 3800 | 1038 | 40000 | 7100 |
| CSF | 0.62 | 4000 | 1007 | 0 | 0 |
| eye (aqueous humor) | 0.58 | 4000 | 1009 | 0 | 0 |
| eye (lens) | 0.40 | 3600 | 1053 | 0 | 0 |
| eye (sclera/wall) | 0.58 | 3800 | 1026 | 75000 | 22000 |
| heart | 0.54 | 3900 | 1030 | 54000 | 9600 |
| liver | 0.51 | 3700 | 1030 | 68000 | 12000 |
| lung (outer) | 0.14 | 3800 | 1050 | 9500 | 1700 |
| kidneys | 0.54 | 4000 | 1050 | 270000 | 48000 |
| intestine (small) | 0.57 | 4000 | 1043 | 71000 | 13000 |
| intestine (large) | 0.56 | 3700 | 1043 | 53000 | 9500 |
| gall bladder | 0.47 | 3900 | 1030 | 9000 | 1600 |
| spleen | 0.54 | 3900 | 1054 | 82000 | 15000 |
| stomach | 0.53 | 4000 | 1050 | 29000 | 5200 |
| pancreas | 0.52 | 4000 | 1045 | 41000 | 7300 |
| blood | 0.56 | 3900 | 1058 | 0 | 0 |
| body fluid | 0.56 | 3900 | 1010 | 0 | 0 |
| bile | 0.55 | 4100 | 1010 | 0 | 0 |
| glands | 0.53 | 3500 | 1050 | 360000 | 64000 |
| bladder | 0.43 | 3200 | 1030 | 9000 | 160 |
| testicles | 0.56 | 3900 | 1044 | 360000 | 64000 |
| lunch | 0.56 | 3900 | 1058 | 0 | 0 |
| adrenals | 0.42 | 3300 | 1050 | 270000 | 48000 |
| Tendon | 0.41 | 3300 | 1040 | 9000 | 1600 |

Table 2. Thermal constants of biological tissues.

$$\int_v A(\mathbf{r})dv = \int_S P_{ins}(\mathbf{r})dS + \int_S H(\mathbf{r},t)(T(\mathbf{r},t) - T_a)dS \tag{6}$$

where $T_a$ is the air temperature. The air temperature was divided into the average room temperature $T_{a1}$ (28°C) and the average body-core temperature $T_{a2}$, corresponding to $H_1$ and $H_2$, respectively.

Insensible water loss is known to be roughly proportional to the basal metabolic rate: 20 ml/kg/day for an adult, 40 ml/kg/day for a 3-year-old child, and 50 ml/kg/day for an 8-month-old child (Margaret *et al*. 1942). For the weight listed in Table 1, the insensible water

| | $P_{ins1}$[W] | $P_{ins2}$[W] | $H_1$[W m$^{-2}$ $^{o}$C] | $H_2$[W m$^{-2}$ $^{o}$C] |
|---|---|---|---|---|
| Female | 20.3 | 8.7 | 4.1 | 26.0 |
| 3 year old | 10.7 | 4.6 | 4.0 | 13.1 |
| 8 month old | 8.9 | 3.8 | 3.9 | 13.3 |

Table 3. Insensible water loss and heat transfer rate in the adult female and 3-year-old and 8-month-old children.

losses in the phantoms of a female adult, a 3-year-old child, and an 8-month-old child are 29 W, 15.3 W, and 12.7 W, respectively. Note that the insensible water loss consists of the loss from skin (70%) and the loss from the lungs through breathing (30%) (Karshlake 1972). The heat loss from the skin to the air $P_{ins1}$ and that from the body-core and internal air $P_{ins2}$ are calculated as listed in Table 3.

For the human body, 80% of the total heat loss is from the skin and 20% is from the internal organs (Nakayama & Iriki 1987). Thus, the heat loss from the skin is 68 W in the adult female, 37.6 W in the 3-year-old child, and 25.6 W in the 8-month-old child. Similarly, the heat loss from the internal organs is 17 W in the adult female, 9.4 W in the 3-year-old child, and 6.4 W in the 8-month-old child. Based on the differences among these values and the insensible water loss presented above, we can obtain the heat transfer coefficients, as listed in Table 3.

In order to validate the thermal parameters listed in Table 3, let us compare the heat transfer coefficients between skin and air obtained here to those reported by Fiala *et al.* (1999). In the study by Fiala *et al.* (1999), the heat transfer coefficient is defined allowing for the heat transfer with insensible water loss. Insensible water loss is not proportional to the difference between body surface temperature and air temperature, as shown by Eq. (3), and therefore should not be represented in the same manner for wide temperature variations. Thus, the equivalent heat transfer coefficient due to insensible water loss was calculated at 28°C. For $P_{ins1}$ as in Table 3, the heat transfer coefficient between the skin and air in the adult female was calculated as 1.7 W/m$^2$/°C. The heat transfer coefficient from the skin to the air, including the insensible heat loss, was obtained as 5.7 W/m$^2$/°C. However, the numeric phantom used in this chapter is descretized by voxels, and thus the surface of the phantom is approximately 1.4 times larger than that of an actual human (Samaras *et al.* 2006). Considering the difference in the surface area, the actual heat transfer coefficient with insensible water loss is 7.8 W/m$^2$/°C, which is well within the uncertain range summarized by Fiala *et al*. (1999).

In Sec. 3, we consider the room temperature of 38°C, in addition to 28°C, in order to allow comparison with the temperatures measured by Tsuzuki et al. (1998). The insensible water loss c assumed to be the same as that at 28°C (Karshlake 1972). The heat transfer coefficient from the skin and air is chosen as 1.4 W/m$^2$/°C (Fiala *et al*. 1999). Since the air velocity in the lung would be the range of 0.5 and 1.0 m/s, the heat transfer coefficient $H_2$ can be estimated as 5 – 10 W/m$^2$/°C (Fiala *et al.* 1999). However, this uncertainty does not influence the computational results in the following discussion, because the difference between the

internal air temperature and the body-core temperature is at most a few degrees, resulting in a marginal contribution to heat transfer between the human and air (see Eq. (3)).

### 2.5 Thermoregulatory Response in Adult and Child

For a temperature elevation above a certain level, the blood perfusion rate was increased in order to carry away excess heat that was produced. The variation of the blood perfusion rate in the skin through vasodilatation is expressed in terms of the temperature elevation in the hypothalamus and the average temperature increase in the skin. The phantom we used in the present study is the same as that used in our previous study (Hirata *et al*. 2007b). The variation of the blood perfusion rate in all tissues except for the skin is marginal. This is because the threshold for activating blood perfusion is the order of 2°C, while the temperature elevation of interest in the present study is at most 1°C, which is the rationale for human protection from RF exposure (ICNIRP, 1998).

Perspiration for the adult is modeled based on formulas presented by Fiala *et al*. (2001). The perspiration coefficients are assumed to depend on the temperature elevation in the skin and/or hypothalamus. An appropriate choice of coefficients could enable us to discuss the uncertainty in the temperature elevation attributed to individual differences in sweat gland development:

$$SW(\mathbf{r},t) = \{W_S(\mathbf{r},t)\Delta T_S(t) + W_H(\mathbf{r},t)(T_H(t) - T_{Ho})\} / S \times 2^{(T(\mathbf{r})-T_0(\mathbf{r}))/10} \tag{7}$$

$$W_s(\mathbf{r},t) = \alpha_{11}\tanh(\beta_{11}T_s(\mathbf{r},t) - T_{so}(\mathbf{r})) - \beta_{10}) + \alpha_{10} \tag{8}$$

$$W_H(\mathbf{r},t) = \alpha_{21}\tanh(\beta_{21}T_s(\mathbf{r},t) - T_{so}(\mathbf{r})) - \beta_{20}) + \alpha_{20} \tag{9}$$

where $S$ is the surface area of the human body, and $W_S$ and $W_H$ are the weighting coefficients for perspiration rate associated with the temperature elevation in the skin and hypothalamus. Fiala *et al.* (2001) determined the coefficients of $\alpha$ and $\beta$ for the average perspiration rate based on measurements by Stolowijk (1971). In addition to the set of coefficients in Fiala *et al*. (2001), we determined the coefficients for adults with higher and lower perspiration rates parametrically (Hirata *et al*. 2007b). In this chapter, we used these sets of parameters.

Thermoregulation in children, on the other hand, has not been adequately investigated yet. In particular, perspiration in children remains unclear (Bar-Or 1980, Tsuzuki *et al*. 1995). Therefore, heat stroke and exhaustion in children remain topics of interest in pediatrics (McLaren *et al*. 2005). Tsuzuki *et al*. (1995) and Tsuzuki (1998) found greater water loss in children than in mothers when exposed to heat stress. Tsuzuki *et al*. (1995) attributed the difference in water loss to differences in maturity level in thermophysiology (See also McLaren *et al*. 2005). However, a straightforward comparison cannot be performed due to physical and physiological differences. A number of studies have examined physiological differences among adults, children, and infants (e.g., Fanaroff *et al*. 1972, Stulyok *et al*. 1973). The threshold temperature for activating perspiration in infants (younger than several weeks of age) is somewhat higher than that for adults (at most 0.3°C). On the other hand, the threshold temperature for activating perspiration in children has not yet been investigated. In the present study, we assume that the threshold temperature for activating perspiration is the same in children and adults. Then, we will discuss the applicability of the

present thermal model of an adult to an 8-month-old child by comparing the computed temperature elevations of the present study with those measured by Tsuzuki (1998).

## 3. Temperature Variation in the Adult and Child Exposed to Hot Room

### 3.1 Computational Temperature Variation in Adult

Our computational result will be compared with those measured by Tsuzuki (1998). The scenario in Tsuzuki (1998) was as follows: 1) resting in a thermoneutral room with temperature of 28°C and a relative humidity of 50%, 2) exposed to a hot room with temperature of 35°C and a relative humidity of 70% for 30 min., and 3) resting in a themoneutral room.

First, the perspiration model of Eq. (7) with the typical perspiration rate defined in Hirata *et al*. (2007b) is used as a fundamental discussion. Figures 2 and 3 show the time course of the average skin and body-core temperature elevations, respectively, in the adult exposed to a hot room, together with those for an 8-month-old child. As shown in Fig. 2, the computed average temperature elevation of the adult skin was 1.5°C for a heat exposure time of 30 min., which is in excellent agreement with the measured data of 1.5°C. From Fig. 3, the measured and computed body-core temperatures in the adult female were 0.16°C and 0.19°C, respectively, which are well within the standard deviation of 0.05°C obtained in the measurement (Tsuzuki 1998). In this exposure scenario, the total water loss for an adult was 50 g/m$^2$ in our computation, whereas it was 60 g/m$^2$ in the measurements.

In order to discuss the uncertainty of temperature elevation due to the perspiration, the temperature elevations in the adult female is calculated for different perspiration parameters given in Hirata *et al*. (2007b). From Table 4(a), the set of typical perspiration parameters works better than other sets for determining the skin temperature. However, the body-core temperature for the typical perspiration rate was larger than that measured by

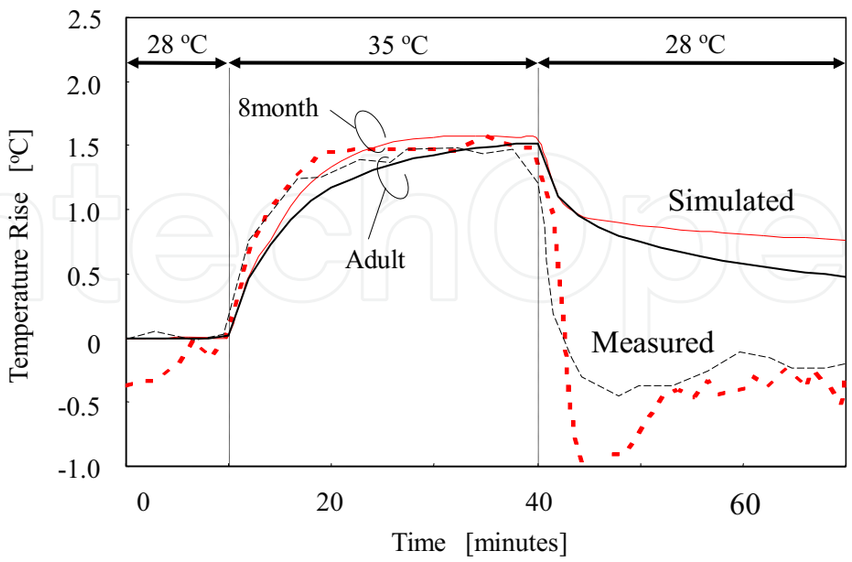


Fig. 2. Time course of average skin temperature elevations in the adult and the 8-month-old child.

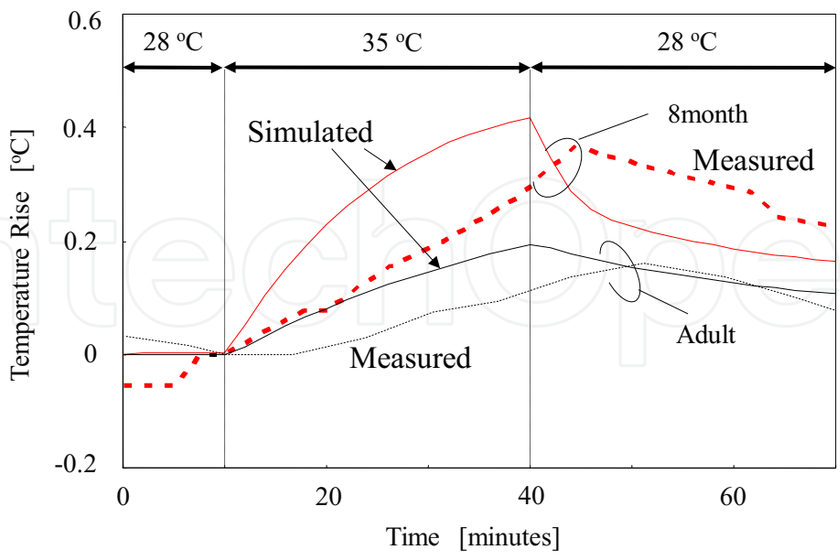


Fig. 3. Time course of body-core temperature elevations in the adult and the 8-month-old child.

| child | low | typical | high | measured |
|---|---|---|---|---|
| skin | 2.0 | 1.5 | 0.98 | 1.5 |
| body-core | 0.50 | 0.41 | 0.32 | 0.37 |

(a)

| adult | low | typical | high | measured |
|---|---|---|---|---|
| skin | 1.7 | 1.5 | 1.2 | 1.5 |
| body-core | 0.21 | 0.19 | 0.17 | 0.16 |

(b)

Table 4. Temperature elevation in (a) adult and (b) child exposed to a hot room for different perspiration parameters.

Tsuzuki (1998). This is thought to be caused by the decrease in body-core temperature before heat exposure (0-10 min. in Fig. 3).

### 3.2 Computational Temperature Variation in Adult

Since thermal physiology in children has not been sufficiently clarified, we adapted the thermal model of the adult to the 8-month-old child for the fundamental discussion. The time courses of the average skin and body-core temperature elevations in the 8-month-old child are shown in Figs. 2 and 3, respectively. As shown in Fig. 2, the computed average temperature elevation of the skin of a child at 30 min. of heat exposure was 1.5°C, which is the same as that for an adult as well as the measured data. The measured and computed

body-core temperatures in the child were 0.37°C and 0.41°C, respectively. This difference of 0.04°C is well within the standard deviation of 0.1°C obtained in the measurement (Tsuzuki 1998). In our computation, the total perspiration of the child was 100 g/m², whereas in the measurements, the value was 120 g/m²; the same tendency was observed for the adult.
Table 4(b) lists the temperature elevations in the 8-month-old child for different perspiration parameters which were the same as we did for the adult. As with the adult, the model with the typical perspiration rate works better than the other models.

### 3.3 Discussion

From Fig. 2, an abrupt temperature decrease in the recovery phase after exposure in a hot room is observed in the measured data but is not observed in the computed data. The reason for this difference is discussed by Tsuzuki (1998), who reported that wet skin is suddenly cooled in a thermoneutral room. This phenomenon cannot be taken into account in our computational modeling or boundary condition (Eqs. (3) and (4)). Such phenomenon would be considered with other boundary conditions, e.g., a formula by Ibrahiem et al (2005). However, this is beyond the scope of the present study, since our concern is on the temperature elevation in the body.
As shown by Fig. 3, the computed body-core temperature increases more quickly than the measured temperature. The time at which the body-core temperature became maximal in the measurement was retarded by 11 min. for the adult female whereas 5 min. for the child. There are two main reasons for this retard. One is caused by our assumption that the blood temperature is spatially constant and varies instantaneously (See Eq. (5)) based on the fact that the blood circulates throughout the body in 1 min. The other reason is that, in the experiment, we consider the blood temperature elevation instead of that in the rectum. The blood temperature in the rectum increases primarily due to blood circulation at an elevated temperature. In Hirata *et al*. (2007b), the temperature elevation in the hypothalamus, which is located in the brain and considerable as body core, was shown to be retarded by a few minutes relative to the blood temperature elevation. The difference of the retard between the adult and the child is attributed to the smaller body dimensions and greater blood perfusion rate of the child compared to those of the adult. The assumption in Eq. (5) was validated for rabbits (Hirata *et al* 2006b), the body dimensions of which are much smaller than those of a human. In addition, the blood perfusion rate of the rabbit is four times greater than that of the human adult, considering the difference in basal metabolic rate (Gordon *et al*. 1976). From this aspect, the thermal computational model developed here works better for the child than for the adult. This retard in the body-core temperature elevation would give a conservative estimation from the standpoint of thermal dosimetry. In the following discussion, we consider not the temperature elevations at a specific time, but rather the peak temperatures for the measured data.
From table 4, we found some difference in total water loss between adult and child. One of the main reasons for this difference is thought to be the difference in race. The volunteers in the study by Tsuzuki (1998) were Japanese, whereas the data used for the computational modeling was based primarily on American individuals (Stolowijk, 1971). Roberts *et al*. (1970) reported that the number of active sweat glands in Korean individuals (similar to Japanese) is 20-30% greater than that in European individuals (similar to American). In addition, the perspiration rate in Japanese individuals is thought to be greater than that in American individuals, which was used to derive the perspiration formula.

Even though we applied a linear scaling when developing the 8-month-old child phantom, its influence on the temperature looks marginal. This is because the body-temperature is mainly determined by the heat balance between the energy produced through metabolic processes, energy exchange with the convection, and the energy storage in the body (Adair and Black 2003, Ebert et al 2005, Hirata et al 2008). Especially, the anatomy of the phantom does not influence from the heat balance equation in the previous studies, suggesting that our approximation of the linear scaling was reasonable.

Tsuzuki et al. (1995) expected a maturity-related difference in themoregulatory response, especially for perspiration, between the adult and the child. The present study revealed two key findings. The first is the difference in the insensible water loss, which was not considered by Tsuzuki et al (1995). The other is the nonlinear perspiration response controlled by the temperature elevations in the skin and body core (Eq. (7)). In addition to these physiological differences, the larger body surface area-to-mass ratio generated more sweat in the child. The computational results of the present study considering these factors are conclusive and are consistent with the measured results.

From the discussion above, the validity of the thermal model for the adult was confirmed. In addition, the thermal model for the 8-month-old child is found to be reasonably the same as that of the adult.

## 4. Body-core Temperature Elevation in Adult and Child for RF Whole-body Exposures

### 4.1 Computational Results for Temperature Elevation for RF Exposures

An anatomically based human phantom is located in free space. As a wave source, a vertically polarized plane wave was considered; the plane wave was thus incident to a human phantom from the front. Female adult and 3-year-old child phantoms are considered in this section. The reason for using the 3-year-old child phantom is that this phantom is more anatomically correct than the 8-month-old child phantom, which was developed for comparison purposes in Section 3.1 simply by reducing the adult phantom.

The whole-body-averaged SAR has two peaks for plane-wave exposure at the ICNIRP reference level; more precisely, it becomes maximal at 70 MHz and 2 GHz in the adult female phantom and 130 MHz and 2 GHz in the 3-year-old child phantom. The first peak is caused by whole-body resonance in the human body. The latter peak, on the other hand, is caused by the relaxation of the ICNIRP reference level with the increase in frequency. Note that the power density at the ICNIRP reference level is 2 W/m$^2$ at 70 MHz and 130 MHz and 10 W/m$^2$ at 2 GHz. The whole-body-averaged SAR in the adult female phantom was 0.069 W/kg at 70 MHz and 0.077 W/kg at 2 GHz, whereas that in the 3-year-old child phantom was 0.084 W/kg at 130 MHz and 0.108 W/kg at 2 GHz. The uncertainty of whole-body SAR, attributed to the boundary conditions and phantom variability, has been discussed elsewhere (e.g., Findlay and Dimbylow 2006, Wang *et al*. 2006, Conil *et al*. 2008). In order to clarify the effect of frequency or the SAR distribution on the body-core temperature, we normalized the whole-body-averaged SAR as 0.08 W/kg while maintaining the SAR distribution. The normalized SAR distributions at these frequencies are illustrated in Fig. 4. As this figure shows, the SAR distributions at these frequencies are quite different (Hirata *et al.* 2007a). EM absorption occurs over the whole body at the resonance frequency. Compared

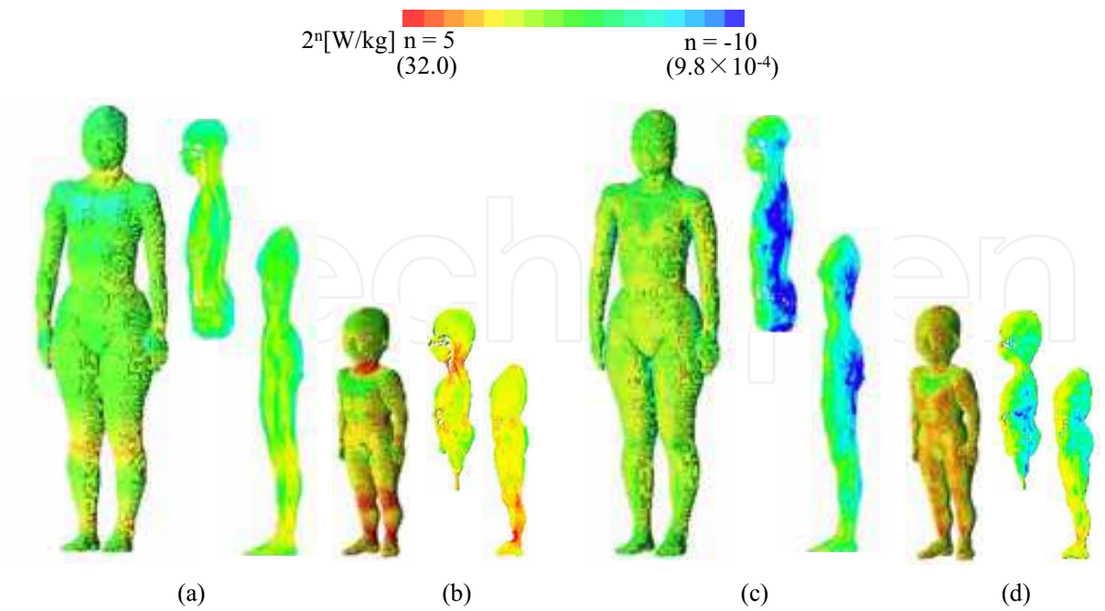


Fig. 4. SAR distributions in the adult female at (a) 70 MHz and (b) 2 GHz and those in the 3-year-old child model at (c) 130 MHz and (d) 2 GHz.

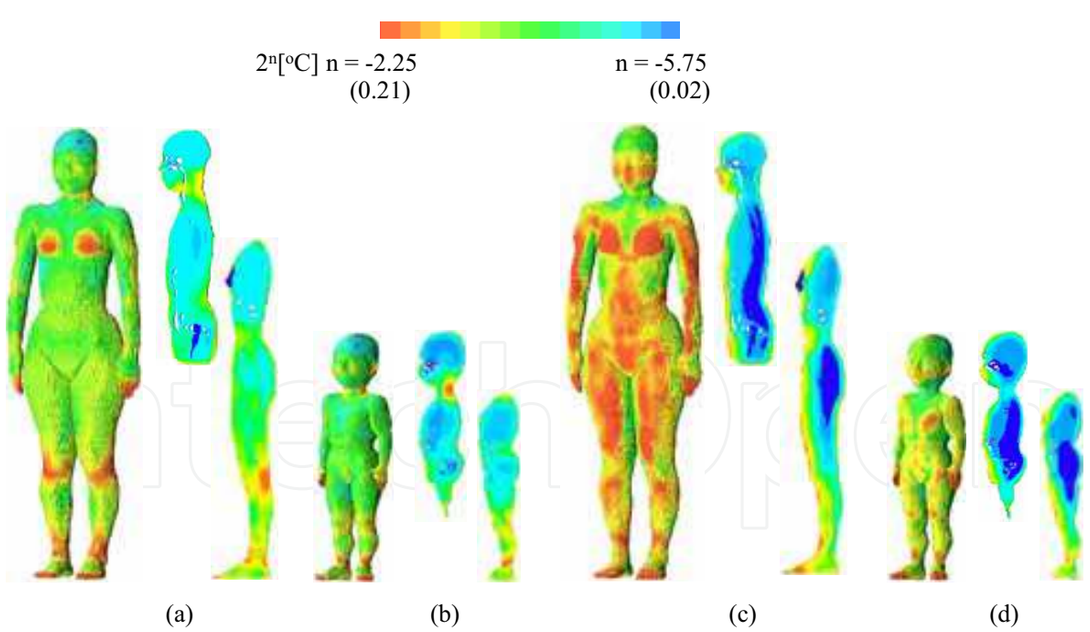


Fig. 5. Temperature elevation distributions in the adult female at (a) 70 MHz and (b) 2 GHz and those in 3-year-old child model at (c) 130 MHz and (d) 2 GHz.

with the distribution at 2 GHz, the absorption around the body core cannot be neglected. In contrast, the SAR distribution is concentrated around the body surface at 2 GHz.

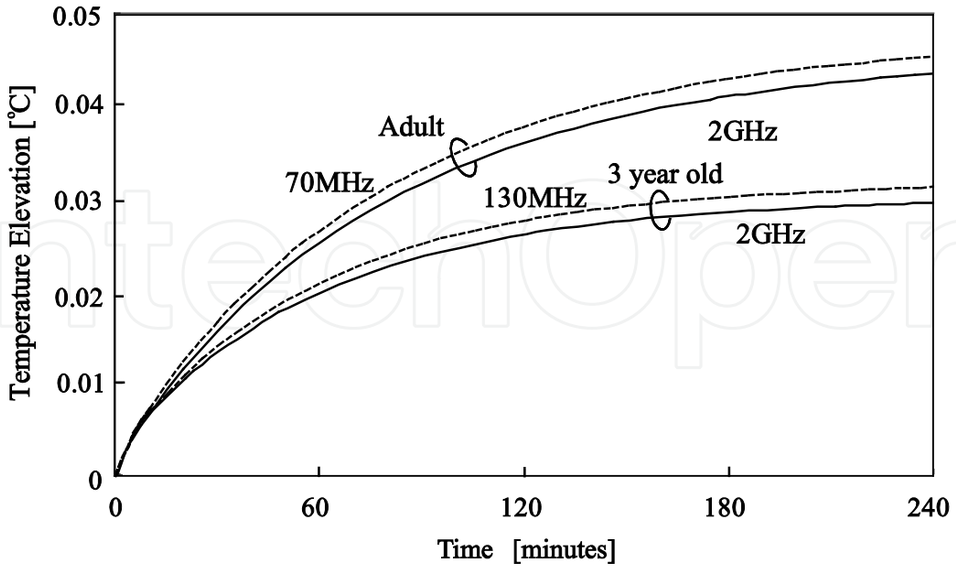


Fig. 6. Temperature elevation in the adult and 3-year-old child at the whole-body averaged SAR of 0.08 W/kg. Exposure duration was 4 hour.

The temperature elevation distributions in a human are illustrated in Fig. 5 for the whole-body-averaged SAR of 0.08 W/kg. The duration of exposure was chosen as 60 min. As shown in Fig. 5, the SAR and temperature elevation distributions are similar. For example, the temperature elevation at the surface becomes larger at 2 GHz. However, the temperature in the body core (e.g., in the brain) is uniform at approximately 0.03°C. This is because the body core is heated mainly due to the circulation of warmed blood (Hirata *et al*. 2007b).
Figure 6 shows the time courses of the temperature elevation in the adult and the child at a whole-body-averaged SAR of 0.08 W/kg. This figure indicates that it took 4 hours to reach the thermally steady state. At 4 hours, the body-core temperature increases by 0.045°C at 65 MHz and 0.041°C at 2 GHz. This confirms the finding in our previous study (Hirata *et al*. 2007b) that whole-body-averaged SAR influences the body-core temperature elevation regardless of the frequency or SAR distribution. On the other hand, the temperature elevation in the child was 0.031°C at 130 MHz and 0.029°C at 2 GHz, which was 35% smaller than that in the adult.

### 4.2 Discussion

We found in Fig. 6 significant difference of body-core temperature elevation between adult and child. In order to clarify the main factor influencing temperature elevation, let us consider an empirical heat balance equation for the human body as given by Adair et al (1998):

$$M + P_{RF} - P_t = P_s \tag{10}$$

where $M$ is the rate at which thermal energy is produced through metabolic processes, $P_{RF}$ is the RF power absorbed in the body, $P_t$ is the rate of heat transfer at the body surface, and $P_S$ is the rate of heat storage in the body.
More specific expression for (10) is given in the following equation based on on (2) and (3).

$$\begin{aligned}&\int_0^t\int_V \big(A(\boldsymbol{r},t)-A(\boldsymbol{r},0)\big)dVdt+\int_0^t\int_V SAR(\boldsymbol{r})\cdot\rho(\boldsymbol{r})dVdt\\&-\left\{\int_0^t\int_S h(\boldsymbol{r})\big(T(\boldsymbol{r},t)-T(\boldsymbol{r},0)\big)dSdt+\int_0^t\int_S SW(t)dSdt\right\}\\&=\int_V\big(T(\boldsymbol{r},t)-T(\boldsymbol{r},0)\big)\cdot\rho(\boldsymbol{r})\cdot C(\boldsymbol{r})dV\end{aligned} \tag{11}$$

The first term of (11) represents the energy due to the metabolic increment caused by the temperature elevation. In this chapter, this term is ignored for the sake of simplicity, since that energy evolves secondarily via the temperature elevation due to RF energy absorption.
For (11), we apply the following two assumptions: 1) the temperature distribution is assumed to be uniform over the body, and 2) the SAR distribution is assumed to be uniform. Then, we obtained the following equation:

$$\begin{aligned}\big(T(t)-T_0\big)\cdot\rho_{WBave}\cdot V\cdot C_{WBave}&=\int_0^t SAR_{WBave}\cdot\rho_{WBave}\cdot Vdt\\&-\int_0^t\big(T(t)-T_0\big)dt\cdot\left\{\int_S H(\mathbf{r})dS+\int_S sw(t)dS\right\}\end{aligned} \tag{12}$$

where $W$ is the weight of the model [kg], $SAR_{WBave}$ is the WBA-SAR[W/kg], $H$ is the mean value of the heat transfer coefficient between the model and air [W/m$^2$ $^o$C], $C_{WBave}$ is the mean value of the specific heat [J/kg $^o$C]. $sw(t)$ is a coefficient identical to $SW(t)$ except that the temperature is assumed to be uniform; $SW(t)=sw(t)(T(t)-T_0)$.
By differentiating (12), the temperature elevation is obtained as

$$T(t)=T_0+\frac{W\cdot SAR_{WBave}}{\int_S H(\vec{r})dS+\int_S sw(t)dS}\left(1-\exp\left(-\frac{\int_S H(\vec{r})dS+\int_S sw(t)dS}{W\cdot C_{WBave}}t\right)\right). \tag{13}$$

As can be seen from Eq. (13), the ratio of surface area to the weight is considered dominant factor influencing the temperature elevation. The total power deposited in the human is proportional to weight, as we fixed the whole-body-averaged SAR as 0.08 W/kg. On the other hand, the power loss from the human via perspiration is proportional to the surface area, because perspiration of the child can be considered as identical to that of the adult. As listed in Table 1, the ratio of the surface to the weight is 0.029 m$^2$/kg for the adult, whereas that of the child is 0.043 m$^2$/kg. This difference of 47% coincides reasonably with the fact that body-core temperature elevation in the child is 35% smaller than that in the adult. Marginal inconsistency in these ratios would be caused by the nonlinear response of the perspiration as given by Eq. (7).
For higher whole-body-averaged SAR( ~ 4 W/kg), the ratio of temperature elevations in the adult to that of the child was 42%, which was closer to their body surface area-to-weight

ratio of 47% than that in the case for the whole-body-averaged SAR at 0.08 W/kg. For higher temperature elevation, the effect of body-core temperature elevation on the perspiration rate is much larger than that due to skin temperature elevation. In addition, the perspiration rate becomes almost saturated. Therefore, the thermal response is considered to be linear with respect to the body-core temperature increase.

It is worth commenting on the difference between this scenario and that described in Section 3.1. In Section 3.1, the body-core temperature elevation in the child was larger than that in the adult for the heat stress caused by higher ambient temperature. The thermal energy applied to the body via ambient temperature is proportional to the surface area of the body. On the other hand, in this scenario, the thermal energy moves from the surface area of the body to the air, because the body is cooled via the ambient temperature. For these two cases, the main factor varying the body-core temperature is the same as the body surface area-to-weight ratio. However, the magnitude relation between the body surface and the ambient temperatures was reversed.

## 5. Conclusion

The temperature elevations in the anatomically-based human phantoms of adult and 3-year-old child were calculated for radio-frequency whole-body exposure. The rationale for this investigation was that further work on thermal dosimetry of children with appropriate thermoregulatory response is listed as one of the high priority researches in the RF research agenda by the WHO (2006). However, systemic work on the difference in the thermoregulation between young child and adult has not been performed, mainly because of ethical reason for experiment and the lack of reliable thermal computational model.

In this chapter, we discussed computational thermal model in the child which is reasonable to simulate body-core temperature elevation in child phantoms by comparing with experimental results of volunteers when exposed to hot ambient temperature. From our computational results, it was found to be reasonable to consider that the thermal response even in the 8-month-old child was almost the same as that in the adult. Based on this finding, we calculated the body-core temperature elevation in the 3-year-old child and adult for plane wave exposure at the ICNIRP basic restriction. The body-core temperature elevation in the 3-year-old child phantom was 40% smaller than that of the adult, which is attributed to the ratio of the body surface area to the mass. This rationale for this difference has been explained by deriving a simple formula for estimating core temperature.

## 6. References

Adair, E. R.; Kelleher, S. A., Mack, G. W. & Morocco, T. S. (1998). Thermophysiological responses of human volunteers during controlled whole-body radio frequency exposure at 450 MHz, *Bioelectromagnetics*, Vol.19, pp. 232-245

Adair, E. R.; Cobb, B. L., Mylacraine, K. S. & Kelleher, S. A. (1999) Human exposure at two radio frequencies (450 and 2450 MHz): Similarities and differences in physiological response, *Bioelectromagnetics*, Vol.20, pp. 12-20

Adair, E. R. & Black, D. R. (2003). Thermoregulatory responses to RF energy absorption, Bioelectromagnetics, Vol.24 (Suppl. 6), pp.S17-S38

American Conference of Government Industrial Hygienists (ACGIH) (1996) Threshold limit values for chemical substances and physical agents and biological exposure indices (Cincinnati OH)

Bar-Or, O.; Dotan, R.; Inbar, O.; Rotshtein, A. & Zonder, H. (1980) Voluntary hypohydration in 10 to 12 year old boys *J. Appl. Physiol.*, Vol.48, pp.104-108

Bernardi, P; Cavagnaro, M.; Pisa, S. & Piuzzi, E. (2003) Specific absorption rate and temperature elevation in a subject exposed in the far-field of radio-frequency sources operating in the 10-900-MHz range *IEEE Trans. Biomed. Eng.*, vol.50, pp. 295-304

Conil, E; Hadjem, A; Lacroux, Wong, M.-F. & Wiart, J. (2008) Variability analysis of SAR from 20 MHz to 2.4 GHz for different adult and child models using finite-difference time-domain *Phys. Med. Biol.* Vol.53, pp. 1511-1525

Cooper, T. E. & Trezek, G. J. (1971) Correlation of thermal properties of some human tissue with water content, *Aerospace Med.*, Vol. 50, pp. 24-27

Chatterjee, I. & Gandhi, O. P. (1983) An inhomogeneous thermal block model of man for the electromagnetic environment *IEEE Trans. Biomed. Eng.*, Vol.30, pp. 707-715

Dimbylow, P. J. (2002). Fine resolution calculations of SAR in the human body for frequencies up to 3 GHz *Phys. Med. Biol.*, Vol.47,pp. 2835-2846

Dimbylow, P. (2005). Resonance behavior of whole-body averaged specific absorption rate (SAR) in the female voxel model, NAOMI. *Phys. Med. Biol.*, vol.50, pp.4053-4063.

Douglas, H. K. (1977) Handbook of Physiology, Sec. 9, Reactions to environmental agents MD: American Physiological Society

Fanaroff, A. A.; Wald, M.; Gruber, H. S. & Klaus, M. H. (1972) Insensible water loss in low birth weight infants *Pediatrics* , Vol. 50, pp. 236-245

Fiala, D.; Lomas, K. J. & Stohrer, M. (1999) A computer model of human thermoregulation for a wide range of environmental conditions: the passive system, *J Appl Physiol*, Vol. 87, pp. 1957-1972

Fiala, D.; Lomas, K. J. & Stohrer, M. (2001) Computer prediction of human thermoregulation and temperature responses to a wide range of environmental conditions, *Int J Biometeorol*, Vol. 45, pp. 143-159

Findlay, R. P. & Dimbylow, P. J. (2006) Variations in calculated SAR with distance to the perfectly matched layer boundary for a human voxel model, *Phys. Med. Biol.*, Vol. 51, pp. N411-N415

Follow, B. & Neil, E. Eds (1971) Circulation, Oxford Univ. Press (New York USA)

Foster, K. R. & Adair, E. R. (2004) Modeling thermal responses in human subjects following extended exposure to radiofrequency energy, *Biomed. Eng. Online* 3:4

Fujimoto, S.; Watanabe, T.; Sakamoto, A.; Yukawa, K. & Morimoto, K. (1968) Studies on the physical surface area of Japanese., 18. Calculation formulas in three stages over all ages. *Nippon Eiseigaku Zasshi*, Vol. 23, pp. 443-450 (in Japanese).

Gabriel, C. (1996) Compilation of the dielectric properties of body tissues at RF and microwave frequencies. Final Tech Rep Occupational and Environmental Health Directorate. AL/OE-TR-1996-0037 (Brooks Air Force Base, TX: RFR Division)

Gordon, R. G.; Roemer, R. B. & Horvath, S. M. (1976) A mathematical model of the human temperature regulatory system-transient cold exposure response *IEEE Trans Biomed Eng*, Vol. 23, pp. 434-444

Hardy, J. D. & DuBois, E. F. (1938) Basal metabolism, radiation, convection, and vaporization at temperatures of 22-35 °C, *J. Nutr.*, Vol. 15, pp. 477-492

Hirata, A.; Fujiwara, O. & Shiozawa, T. (2006a) Correlation between peak spatial-average SAR and temperature increase due to antennas attached to human trunk, *IEEE Trans. Biomed. Eng.*, Vol. 53, pp. 1658-1664

Hirata, A.; Watanabe, S.; Kojima, M.; Hata, I.; Wake, K.; Taki, M.; Sasaki, K.; Fujiwara, O. & Shiozawa, T. (2006b) Computational verification of anesthesia effect on temperature variations in rabbit eyes exposed to 2.45-GHz microwave energy, *Bioelectromagnetics* , Vol. 27, pp. 602-612

Hirata, A. Kodera, S. Wang, J. & Fujiwara, O. (2007a) Dominant factors influencing whole-body average SAR due to far-field exposure in whole-body resonance frequency and GHz regions *Bioelectromagnetics*, Vol. 28, pp.484-487

Hirata, A.; Asano, T. & Fujiwara, O. (2007b) FDTD analysis of human body-core temperature elevation due to RF far-field energy prescribed in ICNIRP guidelines, *Phys Med Biol* , Vol. 52, pp. 5013-5023

Hirata, A. & Fujiwara, O. (2009) Modeling time variation of blood temperature in a bioheat equation and its application to temperature analysis due to RF exposure, *Phys Med Biol* , Vol. 54, pp. N189-196

Hoque, M. & Gandhi, O. P. (1988) Temperature distribution in the human leg for VLF-VHF exposure at the ANSI recommended safety levels, *IEEE Trans. Biomed. Eng.* Vol. 35, pp. 442-449.

Ibrahiem, A.; Dale, C.; Tabbara, W. & Wiart J. (2005) Analysis of temperature increase linked to the power induced by RF source

International Commission on Radiological Protection (ICRP), (1975) Report of the Task Group on Reference Man, Vol.23, Pergamon Press: Oxford.

International Commission on Non-Ionizing Radiation Protection (ICNIRP). (1998) Guidelines for limiting exposure to time-varying electric, magnetic, and electromagnetic fields (up to 300 GHz)., *Health Phys.*, Vol. 74, pp. 494-522

Karslake D. De. K. (1972) The stress of hot environment. Cambridge Univ. Press, London.

Margaret, W.; Johnston, W. & Newburgh, L. H. (1942) Calculation of heat production from insensible loss of weight, *J Clin Invest.*, Vol.21, pp.357–363

Mason, P. A.; Hurt, W. D.; Walter, T. J.; D'Andrea, A.; Gajsek, P.; Ryan, K. L.; Nelson, D.A.; Smith, K. I.; & Ziriax, J. M. (2000) Effects of frequency, permittivity and voxel size on predicted specific absorption rate values in biological tissue during electromagnetic-field exposure. *IEEE Trans. Microwave Theory Tech.,*Vol.48, No. 11, pp-2050-2058.

McLaren, C.; Null, J. & Quinn, J. (2005) Heat stress from enclosed vehicles: moderate ambient temperatures cause significant temperature rise in enclosed vehicles, Vol. 116, pp. e109-e112

Nagaoka, T.; Watanabe, S.; Sakurai, K.; Kunieda, E.; Watanabe, S.; Taki, M. & Yamanaka, Y. (2004) Development of realistic high-resolution whole-body voxel models of Japanese adult males and females of average height and weight, and application of models to radio-frequency electromagnetic-field dosimetry *Phys. Med. Biol.* , Vol. 49, pp. 1-15

Nagaoka, T.; Kunieda, E. & Watanabe, S. (2008) Proportion-corrected scaled voxel models for Japanese children and their application to the numerical dosimetry of specific

absorption rate for frequencies from 30 MHz to 3 GHz, *Phys. Med. Biol.*, Vol. 53, pp.6695-6711

Nakayama, T. & Iriki, M. Ed. (1987) Handbook of Physiological Science vol.18: Physiology of Energy Exchange and Thermoregulation Igaku-Shoin (Tokyo)

Pennes, H. H. (1948) Analysis of tissue and arterial blood temperatures in resting forearm *J. Appl. Physiol.*, Vol. 1, pp. 93-122

Roberts, D.F.; Salzano, F. M. & Willson, J. O. C. (1970) Active sweat gland distribution in caingang Indians *Am. J. Phys. Anthrop.* Vol. 32, pp. 395-400

Samaras, T.; Christ, A. & Kuster, N. (2006) Effects of geometry discretization aspects on the numerical solution of the bioheat transfer equation with the FDTD technique *Phys. Med. Biol.*, Vol. 51, pp. 221-229

Spiegel, R. J. (1984) A review of numerical models for predicting the energy deposition and resultant thermal response of humans exposed to electromagnetic fields *IEEE Trans. Microwave Theory Tech.* Vol.32, pp.730-746

Stolwijk, J. A. J. (1971) A mathematical model of physiological temperature regulation in man. Washington, DC: NASA (CR-1855)

Stulyok, E.; Jequier, E. & Prodhom, L. S. (1973) Respiratory contribution to the thermal balance of the newborn infant under various ambient conditions *Pediatrics*, Vol.51, pp. 641-650

Taflove, A. & Hagness, S. (2003) Computational Electrodynamics: The Finite-Difference Time-Domain Method: 3rd Ed. Norwood. MA: Artech House

Tsuzuki, K.; Tochibara, Y. & Ohnaka, T. (1995) Thermoregulation during heat exposure of young children compared to their mothers, *Eur. J. Appl. Physiol.* Vol. 72, pp. l2-17

Tsuzuki, K. (1998) Thermoregulation during hot and warm exposures of infants compared to their mothers, *Jpn. Soc. Home Economics*, Vol. 49, pp. 409-415

Wang, J; Kodera, S.; Fujiwara, O. & Watanabe, S. (2005) FDTD calculation of whole-body average SAR in adult and child models for frequencies from 30 MHz to 3 GHz *Phys Med Biol*, Vol. 51, pp. 4119-4127

World Health Organization (WHO) (2006) RF research agenda, http://www.who.int/peh-emf/research/rf_research_agenda_2006.pdf


**Recent Advances in Biomedical Engineering**

Edited by Ganesh R Naik

ISBN 978-953-307-004-9
Hard cover, 660 pages
**Publisher** InTech
**Published online** 01, October, 2009
**Published in print edition** October, 2009

The field of biomedical engineering has expanded markedly in the past ten years. This growth is supported by advances in biological science, which have created new opportunities for development of tools for diagnosis and therapy for human disease. The discipline focuses both on development of new biomaterials, analytical methodologies and on the application of concepts drawn from engineering, computing, mathematics, chemical and physical sciences to advance biomedical knowledge while improving the effectiveness and delivery of clinical medicine. Biomedical engineering now encompasses a range of fields of specialization including bioinstrumentation, bioimaging, biomechanics, biomaterials, and biomolecular engineering. Biomedical engineering covers recent advances in the growing field of biomedical technology, instrumentation, and administration. Contributions focus on theoretical and practical problems associated with the development of medical technology; the introduction of new engineering methods into public health; hospitals and patient care; the improvement of diagnosis and therapy; and biomedical information storage and retrieval. The book is directed at engineering students in their final year of undergraduate studies or in their graduate studies. Most undergraduate students majoring in biomedical engineering are faced with a decision, early in their program of study, regarding the field in which they would like to specialize. Each chosen specialty has a specific set of course requirements and is supplemented by wise selection of elective and supporting coursework. Also, many young students of biomedical engineering use independent research projects as a source of inspiration and preparation but have difficulty identifying research areas that are right for them. Therefore, a second goal of this book is to link knowledge of basic science and engineering to fields of specialization and current research. The editor would like to thank the authors, who have committed so much effort to the publication of this work.

**How to reference**

In order to correctly reference this scholarly work, feel free to copy and paste the following:

Akimasa Hirata (2009). Modeling Thermoregulation and Core Temperature in Anatomically-Based Human Models and Its Application to RF Dosimetry, Recent Advances in Biomedical Engineering, Ganesh R Naik (Ed.), ISBN: 978-953-307-004-9, InTech, Available from: http://www.intechopen.com/books/recent-advances-in-biomedical-engineering/modeling-thermoregulation-and-core-temperature-in-anatomically-based-human-models-and-its-applicatio

INTECH
open science | open minds

**InTech Europe**
University Campus STeP Ri

**InTech China**
Unit 405, Office Block, Hotel Equatorial Shanghai

www.intechopen.com

Slavka Krautzeka 83/A
51000 Rijeka, Croatia
Phone: +385 (51) 770 447
Fax: +385 (51) 686 166
www.intechopen.com

No.65, Yan An Road (West), Shanghai, 200040, China
中国上海市延安西路65号上海国际贵都大饭店办公楼405单元
Phone: +86-21-62489820
Fax: +86-21-62489821



IntechOpen

IntechOpen